TISSUE ENGINEERING
Volume 12, Number 7, 2006

Effects of Electromagnetic Stimulation on Calcified Matrix Production by SAOS-2 Cells over a Polyurethane Porous Scaffold

LORENZO FASSINA, M.Sc.,[1] LIVIA VISAI, Ph.D.,[2] FRANCESCO BENAZZO, M.D.,[3] LAURA BENEDETTI, M.Sc.,[4] ALBERTO CALLIGARO, Ph.D.,[4] MARIA GABRIELLA CUSELLA DE ANGELIS, Ph.D.,[4] AURORA FARINA, M.Sc.,[4] VALENTINA MALIARDI, M.Sc.,[4] and GIOVANNI MAGENES, Ph.D.[1]

ABSTRACT

There is increasing interest in designing new biomaterials that could potentially be used in the form of scaffolds as bone substitutes. In this study we used a hydrophobic crosslinked polyurethane in a typical tissue-engineering approach, that is, the seeding and *in vitro* culturing of cells using a porous scaffold. Using an electromagnetic bioreactor (magnetic field intensity, 2 mT; frequency, 75 Hz), we investigated the effect of the electromagnetic stimulation on SAOS-2 human osteoblast proliferation and calcified matrix production. Cell proliferation was twice as high; expression of decorin, osteocalcin, osteopontin, type I collagen, and type III collagen was greater (1.3, 12.2, 12.1, 10.0, and 10.5 times as great, respectively); and calcium deposition was 5 times as great as under static conditions without electromagnetic stimulation. RT-PCR analysis revealed the electromagnetically upregulated transcription specific for decorin, fibronectin, osteocalcin, osteopontin, transforming growth factor-β, type I collagen, and type III collagen. The immunolocalization of the extracellular matrix constituents showed their colocalization in the cell-rich areas. The bioreactor and the polyurethane foam were designed to obtain cell colonization and calcified matrix deposition. This cultured biomaterial could be used, in clinical applications, as an osteoinductive implant for bone repair.

INTRODUCTION

ONE OF THE KEY CHALLENGES in reconstructive bone surgery is to provide living constructs that can integrate with the surrounding tissue. Bone graft substitutes, such as autografts, allografts, xenografts, and biomaterials, have been widely used to heal critical-size long-bone defects and maxillofacial skeleton defects due to trauma, tumor resection, congenital deformity, and tissue degeneration.

The biomaterials used to build three-dimensional (3D) scaffolds for bone tissue engineering are, for instance, hydroxyapatite;[1] partially demineralized bone;[2] biodegradable poly(lactic acid), poly(glycolic acid), and their copolymer poly(lactic acid–glycolic acid);[3] biodegradable porous polymer-ceramic matrices;[4] starch-based polymer matrices;[5] and biodegradable polyurethane foams.[6]

The preceding osteoinductive and osteoconductive biomaterials are ideal for following a typical approach to tissue engineering, an approach that involves the seeding and *in vitro* culturing of cells within a porous scaffold before implantation. The tissue-engineering method is of great importance. To overcome the drawbacks associated with the static culture systems, such as limited diffusion and inhomogeneous cell-matrix distribution, several bioreactors have been designed: a culture system that makes use of 3D microcarrier scaffolds inside a high-aspect-ratio vessel

[1]Dipartimento di Informatica e Sistemistica, University of Pavia, Pavia, Italy.
[2]Dipartimento di Biochimica, University of Pavia, Pavia, Italy.
[3]Dipartimento SMEC, University of Pavia, IRCCS San Matteo, Pavia, Italy.
[4]Dipartimento di Medicina Sperimentale, University of Pavia, Pavia, Italy.

rotating bioreactor[7] and a perfusion bioreactor,[8] for instance. The ideal feature of a bioreactor is that it supplies suitable levels of oxygen, nutrients, cytokines, growth factors, and mechanical stimulation to populate the volume of the bone graft substitute with bone cells and their extracellular matrix.

Nevertheless, following a possible alternative method, an osteoinductive and osteoconductive scaffold could be cultured, only superficially, with bone cells and their extracellular matrix, to further improve a bulk biomaterial suitable to bone tissue engineering. The superficially living construct could be implanted together with the insertion of a vascular pedicle.[9]

In previous work, using a perfusion bioreactor to culture the SAOS-2 osteoblasts, we produced a calcified matrix inside a hydrophobic, non-biodegradable, biointegrable crosslinked polyurethane.[10] In this study, using the same polyurethane and an electromagnetic bioreactor, we attempted to populate the biomaterial surface with a calcified matrix and osteoblasts, in which cell function can be electromagnetically modulated.[11–22]

Gorna and Gogolewski[6,23] have drawn attention to the ideal features of a cancellous bone graft substitute; it should be porous, with interconnected pores of adequate size, allowing for the ingrowth of capillaries and perivascular tissues; it should attract mesenchymal stem cells from the surrounding bone and promote their differentiation into osteoblasts; it should calcify *in vivo*; it should be elastomeric to avoid shear forces at the interface between bone and bone graft substitute; and it should be biodegradable. Nevertheless, some problems may arise when there is not a suitable equilibrium between the material degradation *in vivo* and tissue regeneration.[24]

Although biodegradation is a common requirement for tissue-engineering scaffolds, this work was aimed at an alternative approach to biointegration: *in vivo* integration of a biostable scaffold,[10] a concept derived from non-polymeric scaffolds for osteointegration.[25–27] The use of this polyurethane foam would overcome the possible problems associated with biodegradable polymers, such as degradation kinetics asynchronous with tissue regeneration and adverse reactions to degradation products.

The aim of this work was to investigate the effect of electromagnetic stimulation on SAOS-2 human osteoblast proliferation and on calcified matrix production; using this method, the scaffold, coated with human bone proteins and calcium minerals, could be used in clinical applications as an osteoinductive agent for bone repair.[28]

MATERIALS AND METHODS

Polyurethane foam composition, synthesis, and characterization

Crosslinked polyurethane foam was synthesized and characterized, as previously described.[10] The foam had the following characteristics: density $0.098 \pm 0.002\ g/cm^3$, open porosity $80\% \pm 2\%$, average pore diameter $624\ \mu m$, compressive moduli E_{dry} 9.82 ± 0.40 MPa, and E_{wet} 4.44 ± 0.31 MPa, under dry and in wet conditions, respectively. Cell culture scaffolds ($Ø = 15$ mm and $h = 2$ mm) were cut from the foam using a manual die.

Cells

Human osteosarcoma cell line SAOS-2 was obtained from the American Type Culture Collection (ATCC, HTB85, Rockville, MD). The cells were cultured in McCoy's 5A modified medium with L-glutamine and HEPES (Cambrex Bio Science Baltimore, Inc., Baltimore, MD), supplemented with 15% fetal bovine serum, 2% sodium pyruvate, 1% antibiotics, and 2 osteogenic substances: 10^{-8} M dexamethasone and 10 mM β-glycerophosphate (Sigma-Aldrich, Inc., Milwaukee, WI). Ascorbic acid, another osteogenic supplement, is a component of McCoy's 5A modified medium. The cells were cultured at 37°C with 5% carbon dioxide (CO_2), routinely trypsinized, counted, and seeded onto the porous polyurethane scaffolds.

Cell seeding

The scaffolds were sterilized with ethylene oxide at 38°C for 8 h at 65% relative humidity.[29] After a 24-h aeration to remove the residual ethylene oxide, the scaffolds were placed inside the 2 culture systems: the static culture system (a standard well-plate far from the electromagnetic bioreactor) and the dynamic or electromagnetic culture system (a standard well-plate inside the electromagnetic bioreactor). A cell suspension of 1×10^6 cells in 400 μL was added onto the top of each scaffold, and after 0.5 h, 1 mL of culture medium was added to cover the scaffolds. Cells were allowed to attach overnight, then the static culture continued in the standard well-plate far from the electromagnetic bioreactor, and the electromagnetic bioreactor was turned on.

Electromagnetic bioreactor

An electromagnetic bioreactor, consisting of a carrying structure custom-machined in a tube of polymethylmethacrylate, was built (Fig. 1A). The windowed tube carried a well-plate and 2 solenoids (i.e., Helmoltz coils, the planes of which were parallel). The surfaces of the polyurethane scaffolds were 5 cm away from each solenoid plane. In this experimental set-up, the magnetic field and the induced electric field were perpendicular and parallel to the scaffold surfaces, respectively.

The solenoids were powered using a Biostim SPT pulse generator (Igea, Carpi, Italy), a pulsed electromagnetic field (PEMF) generator. The electromagnetic bioreactor applied a PEMF to the cells on the scaffold surface with the following characteristics: intensity of the magnetic field 2 ± 0.2 mT, amplitude of the induced electric tension 5 ± 1 mV, signal frequency 75 ± 2 Hz, and pulse duration

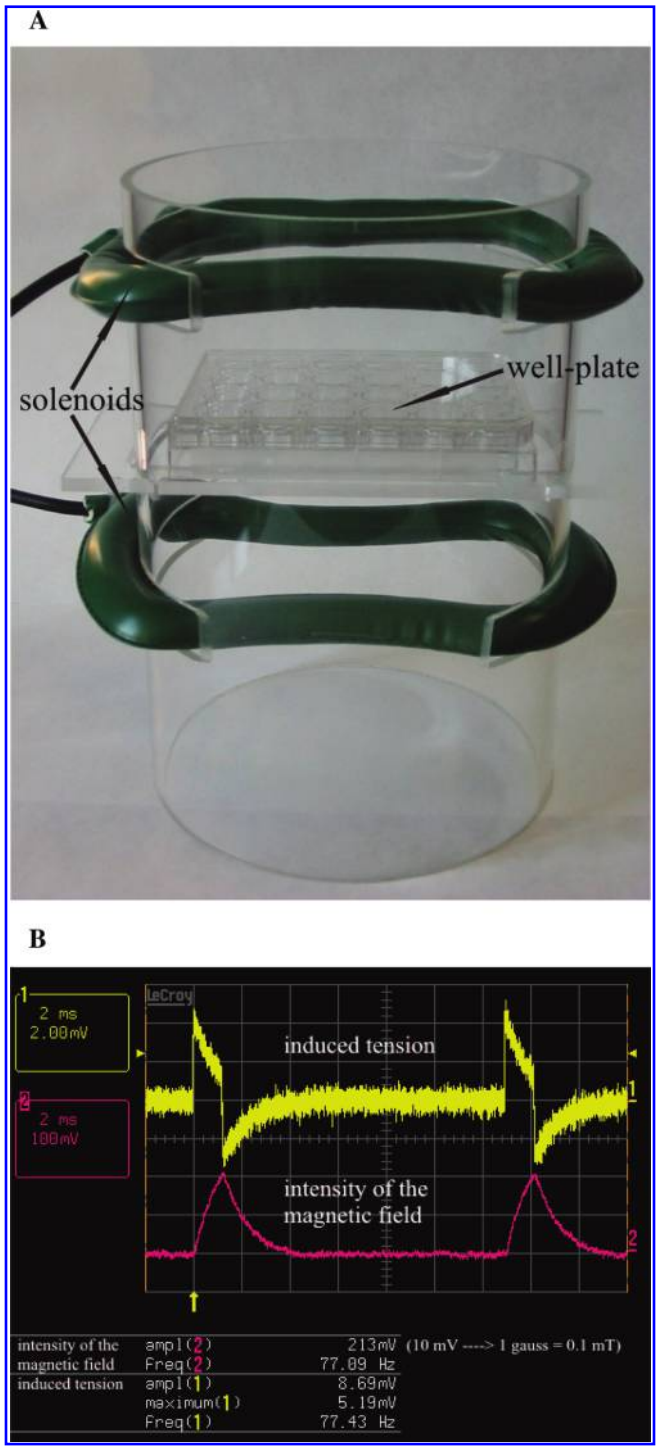

FIG. 1. Electromagnetic bioreactor (**A**) and temporal pattern of the electromagnetic signal (**B**). (Color images available online at www.liebertpub.com/ten.)

approximately 1.3 ms (Fig. 1B). The magnetic field was measured using a Hall Effect transverse gaussmeter probe (catalog no. HTD61-0608-05-T, F.W. Bell line, Sypris Solutions, Inc., Louisville, KY) and a gaussmeter (catalog no. DG-500, Laboratorio Elettrofisico, Milan, Italy), the induced electric tension was measured using a standard coil probe, and the temporal pattern of the electromagnetic signal was evaluated using a digital oscilloscope (catalog no. LT322, WaveRunner Series, LeCroy, Inc., Chestnut Ridge, NY).

The electromagnetic bioreactor was placed in a standard cell-culture incubator at 37°C and 5% CO_2. The dynamic culture was stimulated using the PEMF 24 h/day for 22 days. The culture medium was changed on days 4, 7, 10, 13, 16, and 19, and the conditioned culture medium was sampled for analysis on days 4, 7, 10, 13, 16, 19, and 22.

Standard well-plate culture

The static culture was placed in a different incubator, where the PEMF stimulation was not detectable. The seeded polyurethane scaffolds were simply covered with fresh medium on days 4, 7, 10, 13, 16, and 19, and the conditioned culture medium was sampled for analysis on days 4, 7, 10, 13, 16, 19, and 22.

Light microscopy analysis for histology and for calcium content detection

At the end of the culture period, the scaffolds were fixed with 4% (w/v) paraformaldehyde solution in 0.1 M phosphate buffer (pH = 7.4) for 8 h at room temperature, washed with phosphate buffer, dehydrated in a gradient ethanol series up to 100%, and embedded in paraffin. The histological sections, with 10-μm thickness, were cut orthogonally to the scaffold axis and stained with hematoxylin-eosin or using the von Kossa method (catalog no. 04-170801, Bio-Optica, Milan, Italy). Images were taken using a standard light microscope (Leica Microsystems, Bensheim, Germany) equipped with a digital image capture system (Canon, Inc., Tokyo, Japan) at 400× magnification. The von Kossa staining substitutes calcified matrix calcium^{2+} (Ca^{2+}) ions with silver atoms, coloring the calcified matrix brown; "brown" was defined, on the red-green-blue (RGB) scale, as [R = 120 ÷ 160; G = 60 ÷ 120; B = 40 ÷ 100]. The ratio between the brown region and total image area was measured using ImageJ (http://rsb.info.nih.gov/ij), and a comparison was performed between the dynamic culture and the static culture.

Scanning electron microscopy (SEM) analysis

At the end of the culture period, the scaffolds were fixed with 2.5% (v/v) glutaraldehyde solution in 0.1 M sodium cacodylate buffer (pH = 7.2) for 1 h at 4°C, washed with sodium cacodylate buffer, and then dehydrated at room temperature in a gradient ethanol series up to 100%. The samples were kept in 100% ethanol for 15 min and then critical point–dried using CO_2. The specimens were mounted on aluminum stubs, sputter-coated with gold (degree of purity 99%), and then observed using a Leica Cambridge Stereoscan 440 microscope at 8 kV. The unseeded scaffolds were observed at 18× magnification and the cultured scaffolds at 300× and 600× magnifications.

DNA content

The cells were lysed using a freeze-thaw method in sterile deionized distilled water. The released deoxyribonucleic acid (DNA) content was evaluated using a fluorometric DNA quantification kit (PicoGreen, Molecular Probes, Eugene, OR). A DNA standard curve, obtained from a known amount of osteoblasts, was used to express the results as cell number per scaffold.

Assay for gene transcription

At the end of the culture period, total ribonucleic acid (RNA) was extracted from the cultured scaffolds using the RNeasy system, according to manufacturer's protocol (Qiagen, Inc., Hilden, Germany). Reverse transcriptase–polymerase chain reaction (RT-PCR) was performed to evaluate the transcription specifically for decorin, fibronectin, osteocalcin, osteopontin, transforming growth factor-β (TGF-β), type I collagen, type III collagen, and the housekeeping transcription specific for glyceraldehyde-3-phosphate dehydrogenase. The reverse transcriptase reaction was performed using 500 ng of RNA with the ThermoScript RT-PCR System (Invitrogen Corporation, Carlsbad, CA). The primers (Primm, Milan, Italy) were designed according to the published gene sequences, and the polymerase chain reactions were performed using the GeneAmp PCR System 9700 (Applied Biosystems, Inc., Foster City, CA). The primers were as follows.

Decorin: upstream primer 5′-CGAGTGGTCCAGTGTTCTGA-3′ and downstream primer 5′-AAAGCCCCATTTTCAATTCC-3′, expected product size 360 bp.[30]

Fibronectin: upstream primer 5′-TGGAACTTCTACCAGTGCGAC-3′ and downstream primer 5′-TGTCTTCCCATCATCGTAACAC-3′, expected product size 500 bp.[31]

Osteocalcin: upstream primer 5′-GGCAGCGAGGTAGTGAAGAG-3′ and downstream primer 5′-CTGGAGAGGAGCAGAACTGG-3′, expected product size 230 bp.[32]

Osteopontin: upstream primer 5′-TCACTGATTTTCCCACGGAC-3′ and downstream primer 5′-TCATAACTGTCCTTCCCACG-3′, expected product size 280 bp.[33]

TGF-β: upstream primer 5′-GTGCGGCAGCTCTACATTGACT-3′ and downstream primer 5′-TTGCGGCCCACGTAGTACAC-3′, expected product size 230 bp.[34]

Type I collagen: upstream primer 5′-TGTAAGCGGTGGTGGTTATG-3′ and downstream primer 5′-GGTAGCCATTTCCTTGGAAG-3′, expected product size 450 bp.[35]

Type III collagen: upstream primer 5′-TGGATCAGATGGTCTTCCA-3′ and downstream primer 5′-TCTCCATAATACGGGGCAA-3′, expected product size 620 bp.[36]

The polymerase chain reactions were performed using 2 μL of the complementary DNA mixture using the Platinum Taq DNA Polymerase (Invitrogen Corporation); 30 cycles were run at 94°C for 45 s (denaturation), at 58°C for 45 s (annealing), and at 72°C for 1 min (extension). The transcription specific for all proteins was normalized to the housekeeping transcription specific for glyceraldehyde-3-phosphate dehydrogenase.[37] To obtain a specificity control, the same polymerase chain reactions were performed from 2 μL of the total RNA mixture without the reverse transcriptase reaction. The resulting products were fractionized using electrophoresis through an ethidium bromide–stained 1% agarose gel in 1× Tris-borate ethylenediaminetetraacetic acid buffer. Images were taken using a Kodak DC120 Zoom Digital Camera (Eastman Kodak Company, Rochester, NY).

Set of rabbit polyclonal antisera

Larry Fisher (National Institutes of Health, National Institute of Dental and Craniofacial Research, Craniofacial and Skeletal Diseases Branch, Matrix Biochemistry Unit, Bethesda, MD) presented us, generously, with the following rabbit polyclonal antibody immunoglobulins G (IgGs): anti-osteocalcin, anti-type I collagen, anti-type III collagen, anti-decorin, and anti-osteopontin (antiserum no. LF-32, LF-67, LF-71, LF-136, and LF-166, respectively, http://csdb.nidcr.nih.gov/csdb/antisera.htm).[38–40]

Set of purified proteins

Decorin,[41] osteocalcin (immunoenzymatic assay kit, catalog no. BT-480, Biomedical Technologies, Inc., Stoughton, MA), osteopontin (immunoenzymatic assay kit, catalog no. 900-27, Assay Designs, Inc., Ann Arbor, MI), type I collagen,[42] and type III collagen (Sigma-Aldrich, Inc.).

Immunohistochemistry

At the end of the culture period, the scaffolds were fixed with 4% (w/v) paraformaldehyde solution in 0.1 M phosphate buffer (pH = 7.4) for 8 h at room temperature, washed with phosphate buffer, dehydrated in a gradient ethanol series up to 100%, and embedded in paraffin. The sections, with 10-μm thickness, were cut orthogonally to the scaffold axis, deparaffinized, rehydrated, and processed for the immunohistochemical detection of decorin, osteocalcin, osteopontin, type I collagen, and type III collagen using the avidin-biotin-peroxidase method.[43] Larry Fisher's anti-decorin, anti-osteocalcin, anti-osteopontin, anti-type I collagen, and anti-type III collagen rabbit polyclonal antisera were used as primary antibody, with a dilution equal to 1:4000, 1:2000, 1:2000, 1:2000, and 1:4000, respectively. The sections were treated with 0.3% (v/v) hydrogen peroxide for 30 min at room temperature to inactivate the endogenous peroxidases, washed with Tris buffer saline (TBS) (0.05 M Tris-hydrochloride, 0.15 M sodium chloride, pH = 7.4), blocked by incubating with 10% normal goat serum for 30 min at room temperature, and then washed. The incubation with the primary antibodies was performed overnight at 4°C, whereas the negative controls were based

upon the incubation, overnight at 4°C, with TBS or with rabbit serum instead of the primary antibodies. The sections were washed, incubated with biotinylated goat anti-rabbit IgG (Super Sensitive Link-Label Detection System, BioGenex Laboratories, Inc., San Ramon, CA) for 1 h at room temperature, washed, exposed to horseradish peroxidase–labeled streptavidin for 1 h at room temperature, and then washed. The immunolocalization of the extracellular matrix proteins was performed using 0.03% (v/v) 3,3′-diaminobenzidine tetrahydrochloride with 0.02% (v/v) hydrogen peroxide for 5 min at room temperature. Each solution of the staining procedure was prepared in TBS. The sections were dehydrated, and the images were taken with a standard light microscope (Leica Microsystems) equipped with a digital image capture system (Canon, Inc.) at 400× magnification.

Extraction of the extracellular matrix proteins from the cultured polyurethane scaffolds

At the end of the culture period, to evaluate the amount of the extracellular matrix constituents over the scaffold surface, the scaffolds were washed extensively with sterile PBS (137 mM NaCl, 2.7 mM potassium chloride, 4.3 mM disodium hydrogen phosphate dodecahydrate, 1.4 mM potassium dihydrogen phosphate, pH = 7.4) to remove the culture medium, and then incubated for 24 h at 37°C with 1 mL of sterile sample buffer (1.5 M Tris-hydrochloride, 60% [w/v] sucrose, 0.8% [w/v] sodium dodecyl sulphate, pH = 8.0). At the end of the incubation period, the sample buffer aliquots were removed, and the scaffolds were centrifuged at 4000 rpm for 15 min to collect the sample buffer entrapped in the pores. The total protein concentration, in the static and the dynamic culture systems, was evaluated using the BCA Protein Assay Kit (catalog no. 23227, Pierce Biotechnology, Inc., Rockford, IL). The total protein concentration was 1900 ± 105 μg/mL in the static culture and 2800 ± 141 μg/mL in the dynamic culture, with $p < 0.05$. After matrix extraction, the polyurethane scaffolds were incubated once again for 24 h at 37°C with 1 mL sterile sample buffer, and no protein content was detected.

Enzyme-linked immunosorbent assay (ELISA) of the extracted extracellular matrix

Calibration curves to measure decorin, osteocalcin, osteopontin, type I collagen, and type III collagen were performed. Microtiter wells were coated with increasing concentrations of each purified protein, from 1 ng to 2 μg, in coating buffer (50 mM disodium carbonate, pH = 9.5) overnight at 4°C. Some of the wells were coated with bovine serum albumin (BSA) as a negative control. To measure the extracellular matrix amount of each protein using an ELISA, microtiter wells were coated overnight at 4°C with 100 μL of the extracted extracellular matrix (20 μg/mL in coating buffer). After 3 washes with PBS containing 0.1% (v/v) Tween 20, the wells were blocked by incubating with 200 μL of PBS containing 2% (w/v) BSA for 2 h at 22°C. The wells were subsequently incubated for 1.5 h at 22°C with 100 μL of Larry Fisher's anti-osteocalcin, anti-osteopontin, anti-type I collagen, and anti-type III collagen rabbit polyclonal antisera and with 100 μL of the anti-decorin mouse polyclonal antiserum[10] (1:500 dilution in 1% BSA). After washing, the wells were incubated for 1 h at 22°C with 100 μL of horseradish peroxidase–conjugated goat anti-rabbit IgG or rabbit anti-mouse IgG (1:1000 dilution in 1% BSA). The wells were finally incubated with 100 μL of development solution (phosphate-citrate buffer containing *o*-phenylenediamine dihydrochloride substrate). The color reaction was stopped with 100 μL of 0.5 M sulfuric acid and the absorbance values were measured at 490 nm with a microplate reader (Bio-Rad Laboratories, Inc., Hercules, CA). The results are expressed as fg/(cell×scaffold).

ELISA of the conditioned culture medium

To evaluate the temporal pattern of matrix protein secretion during the culture period, the conditioned medium was sampled as described above and analyzed using ELISA. Anti-decorin mouse polyclonal antiserum[10] and Larry Fisher's anti-type I and anti-type III collagen rabbit polyclonal antisera were used, and the assay procedure was performed as above. The secretions of osteocalcin and osteopontin were measured using commercial immunoenzymatic assay kits as previously described.[10] Protein secretions are expressed as fg/(cell×scaffold). An asymptotic growth model

$$y = a(1 - e^{-bx})$$

was applied, using Matlab (The MathWorks, Inc.), to the total secretion data of decorin and type I collagen measured from both culture systems.

Statistics

The results are expressed as mean ± standard deviation. To compare the results of the static and the dynamic systems, a one-way analysis of variance with *post hoc* Bonferroni test was applied, with a significance level of 0.05.

RESULTS

The osteoblasts were seeded onto the surface of polyurethane porous scaffolds and then cultured in an electromagnetic bioreactor for 22 days. This culture system permitted the study of the SAOS-2 cells as they proliferated and produced a calcified extracellular matrix in an electromagnetically active environment. We compared the cell-matrix distribution and the calcified matrix production of the 2 culture systems.

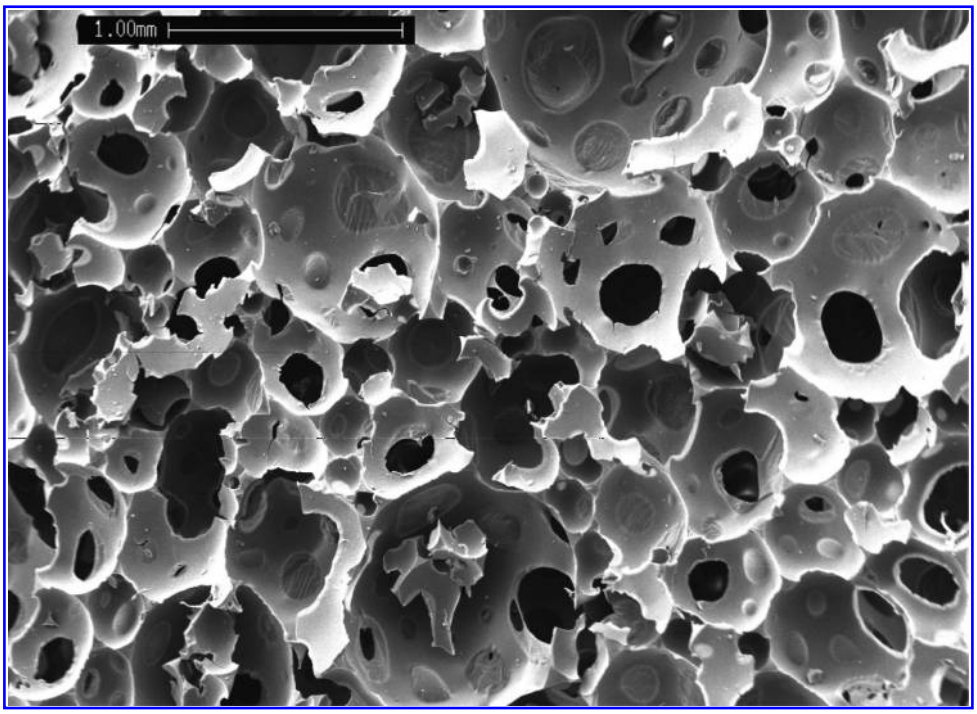

FIG. 2. Scanning electron microscopy observation of an unseeded polyurethane scaffold at 18× magnification.

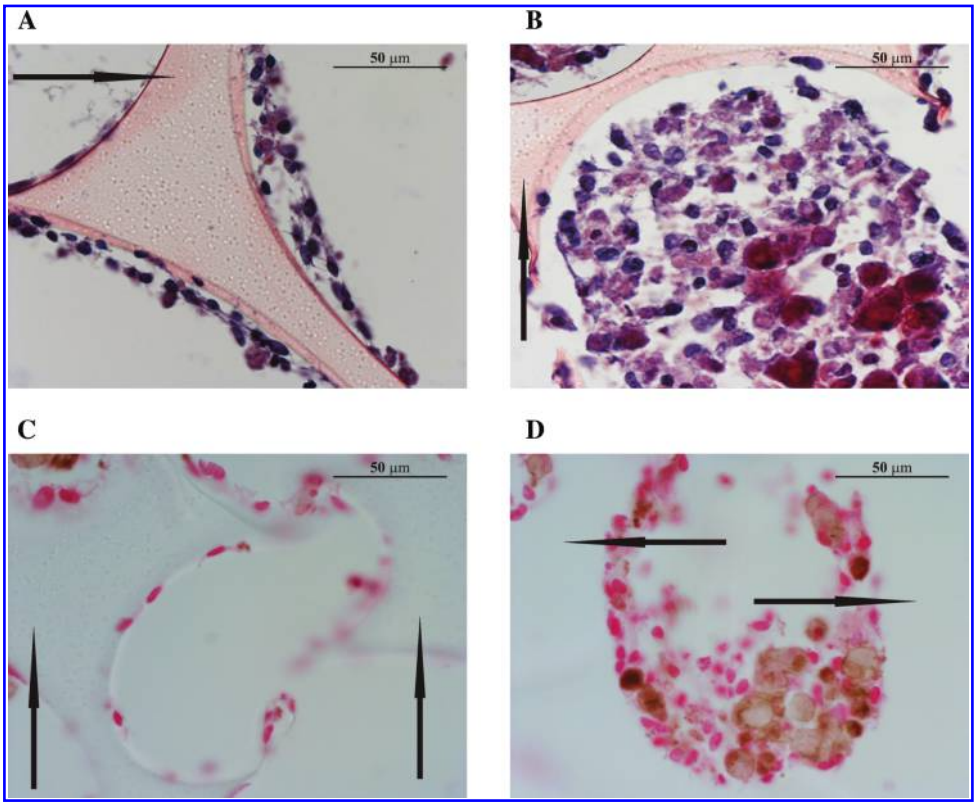

FIG. 3. Histological sections of the static culture (**A**) and of the dynamic culture (**B**), hematoxylin-eosin staining at the end of the culture period, 400× magnification; histological sections of the static culture (**C**) and of the dynamic culture (**D**), von Kossa staining at the end of the culture period, 400× magnification; the osteoblast layers adhered to the polyurethane scaffolds (arrows). (Color images available online at www.liebertpub.com/ten.)

Light microscope and SEM analyses

Using SEM observation, the scaffold morphology appeared uniform, with interconnected pores and smooth pore surfaces (Fig. 2).

The histological sections and the SEM images revealed that, because of the electromagnetic stimulation, the cells proliferated over the available polyurethane surface (Fig. 3, 4). Statically cultured cells were few and were essentially organized in a monolayer with a thin discontinuous extracellular matrix (Fig. 3A, C, 4A, B), whereas the electromagnetic stimulation induced a 3D modeling of the cell-matrix organization; several cells coated the available polyurethane surface in a multilayer, with the volume of the surface pores tending to be filled by cell-matrix clusters growing from the pore bottom (Fig. 3B, D, 4C, D).

These observations were confirmed by measuring the DNA content after 22 days of culture; in the static culture, the cell number per scaffold grew to $18.7\times10^6 \pm 8.2\times10^4$ and in the dynamic culture to $36.3\times10^6 \pm 8.4\times10^4$, with $p < 0.05$. Because the DNA may remain entrapped in the calcified matrix, an underestimation of culture cellularity is possible.

Calcified matrix production

The relative amount of the calcium contained in the scaffolds was quantified to evaluate the matrix calcification (Fig. 3C, D). The von Kossa staining revealed the calcified matrix as brown regions localized in the cell-rich areas, and the ratio between the brown area and the total image area was $2.05\% \pm 0.71\%$ in the static culture and $10.18\% \pm 3.74\%$ in the dynamic; matrix calcification was approximately 5 times as great with electromagnetic stimulation, with $p < 0.05$. No ectopic calcification was observed in either culture system.

Matrix production from RNA to the extracellular space

The analysis of the transcripts specific for decorin, osteocalcin, osteopontin, type I collagen, and type III collagen

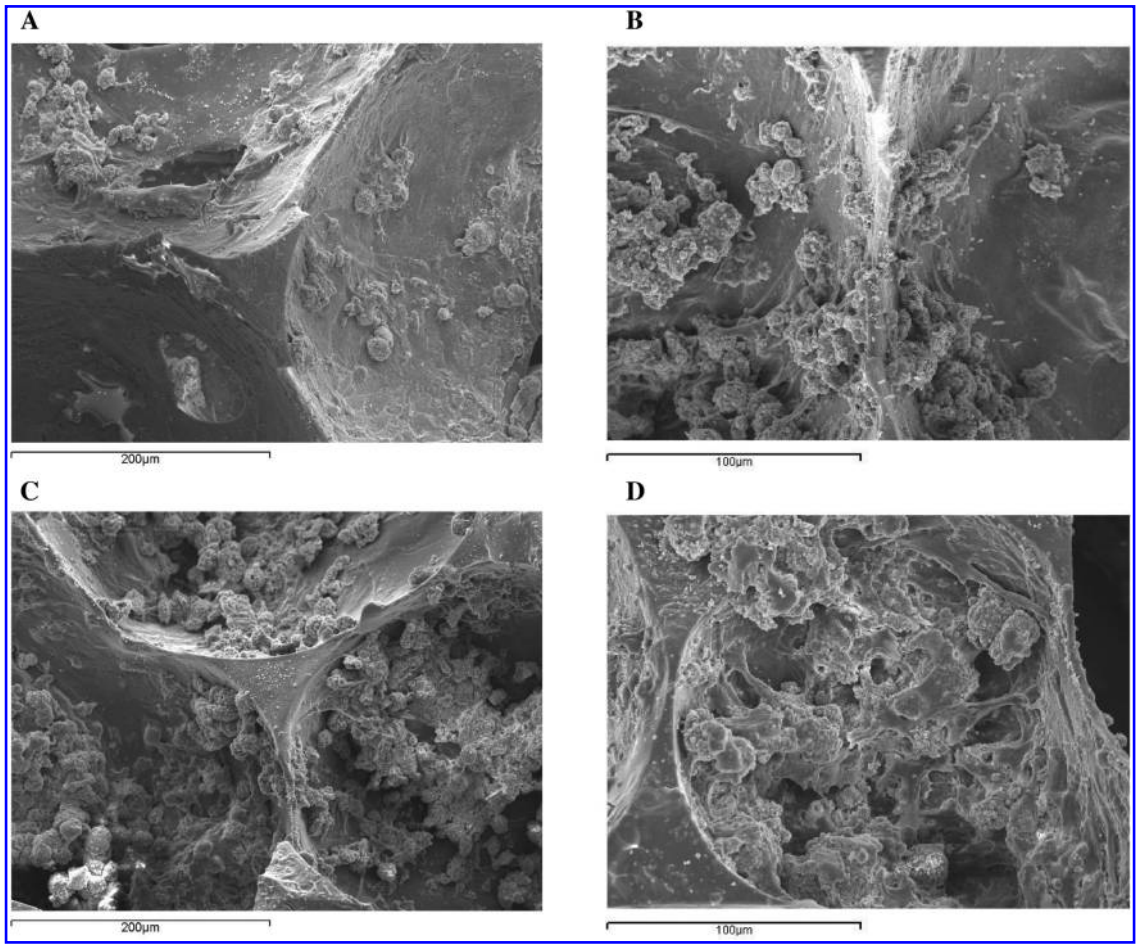

FIG. 4. Scanning electron microscopy observations of the static culture (**A**, **B**) and of the dynamic culture (**C**, **D**) at the end of the culture period, 300× magnification (**A**, **C**) and 600× magnification (**B**, **D**).

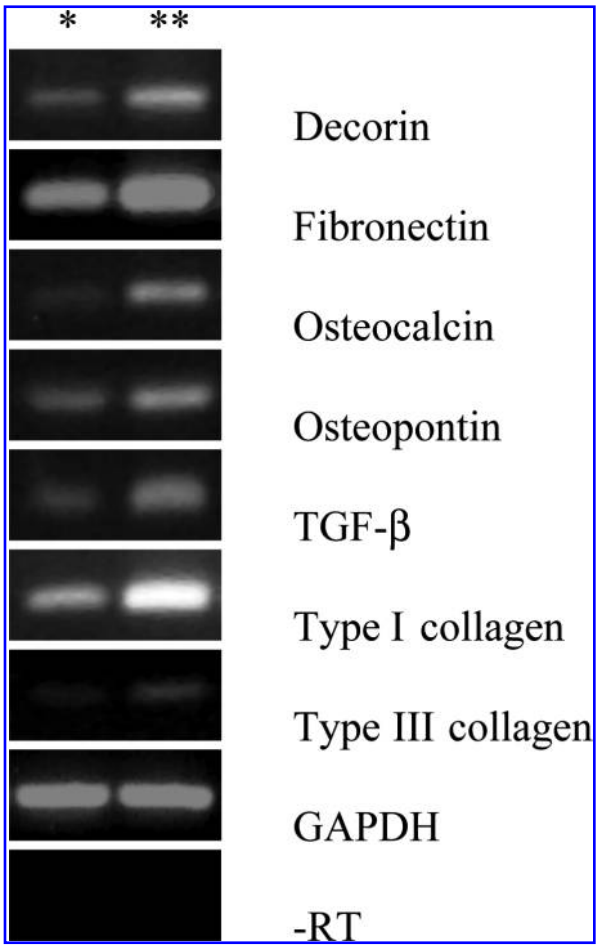

FIG. 5. Assay for gene transcription of the static culture (column*) and of the dynamic culture (column**).

revealed that the application of the electromagnetic wave caused greater transcription than the static culture (Fig. 5).

The immunolocalization of decorin (Fig. 6A, B), osteopontin (Fig. 6C, D), and type I collagen (Fig. 6E, F) showed an intense intracellular and extracellular staining of the cell-rich areas in both culture systems. The immunolocalization of osteocalcin and type III collagen was similar (data not shown). These observations were in agreement with the previous microscope observations (Fig. 3, 4).

To evaluate the amount of the extracellular matrix constituents over the scaffold surface, an ELISA of the extracted matrix was performed; at the end of the culture period, the electromagnetic stimulation increased the coating with bone proteins much more than with the static culture (Table 1). An underestimation of absolute protein deposition is possible because the sample buffer, used for matrix extraction, contained sodium dodecyl sulphate, which may interfere with protein adsorption during ELISA. These measures were in accordance with the microscope images of the extracellular matrix (Fig. 3, 4, 6).

The analysis of the transcripts showed that the electromagnetic bioreactor caused a transcription rise of fibronectin and TGF-β (Fig. 5).

Matrix protein secretion in the culture medium

Decorin, osteocalcin, osteopontin, type I collagen, and type III collagen were detected in both culture systems; nevertheless, after 22 days of culture (after the whole culture period), higher total secretions were found in the dynamically conditioned medium, with $p < 0.05$ (Table 2).

As regards each culture system, to evaluate the split of decorin, osteocalcin, osteopontin, type I collagen, and type III collagen between the scaffold surface and the culture medium, a comparison was made between the amount over the scaffold surface and the total secretion in the culture medium after the whole culture period; the total secretion in the culture medium was considerably lower than the surface amount, with $p < 0.001$ (Table 1, 2).

During the culture period, the secretions of decorin and type I collagen showed an exponentially decreasing temporal pattern in both culture systems, and at each medium change, the comparison between the static and the dynamic systems was characterized by $p < 0.05$ (Fig. 7A, 8A). The asymptotic growth model was applied to the total secretions of decorin and type I collagen with $R^2 > 0.99$ (Fig. 7B, 8B). Similar results were obtained with regard to osteopontin and type III collagen (data not shown).

During the culture period, the secretion of osteocalcin showed a rise-and-fall temporal pattern in both culture systems, with an expression peak between days 7 and 10 in the static culture, whereas between days 4 and 7 in the dynamic culture; at each medium change, the difference between the static and the dynamic systems was significant with $p < 0.05$ (Fig. 9).

DISCUSSION

The aim of this study was the coating of a biomaterial with calcified matrix and osteoblasts to make a biostable polyurethane more suitable to bone repair.

To enhance the culture of human cell line SAOS-2 over the bulk polyurethane, an electromagnetic wave was applied to the seeded scaffolds; *in vivo* experiments demonstrated that a continuous exposure for 30 days to a pulsed electromagnetic field, similar to that used in this study, stimulates bone repair in the healing process of transcortical holes in adult horses.[44]

Electromagnetic stimulation increased the cell proliferation approximately 2 times, and enhanced the gene transcription specific for TGF-β. These results were consistent with the rise in proliferation,[45] growth factor,[19,21] and prostaglandin[19] secretion, and in growth factor receptor number[46] in response to an electromagnetic wave exposure.

A temporal and functional pattern of the gene expression characterizes the osteoblast maturation process, which can

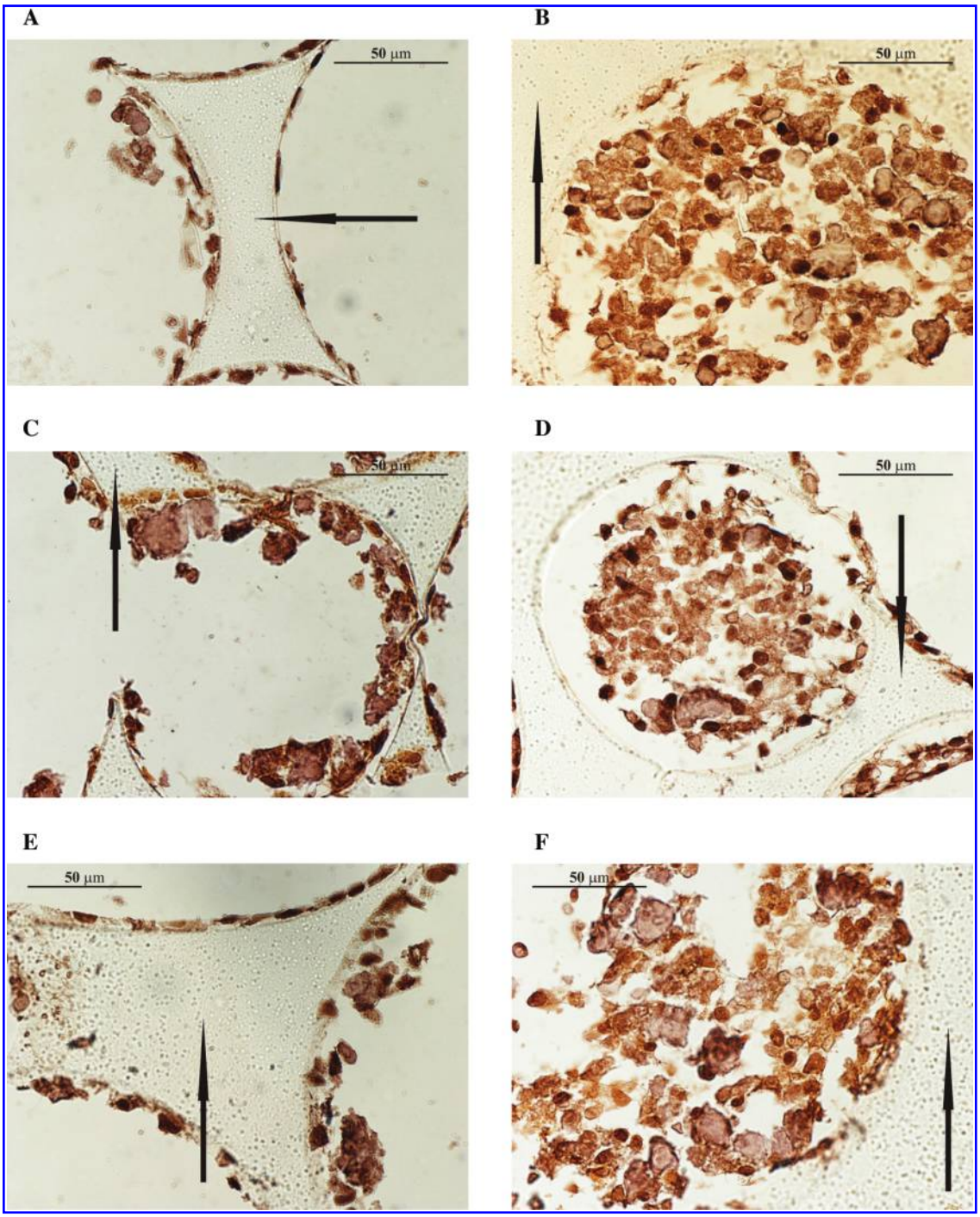

FIG. 6. Immunolocalization of decorin (**A**, **B**), osteopontin (**C**, **D**), and type I collagen (**E**, **F**) in the static culture (**A**, **C**, **E**) and in the dynamic culture (**B**, **D**, **F**) at the end of the culture period, 400× magnification; the osteoblast layers adhered to the polyurethane scaffolds (arrows). (Color images available online at www.liebertpub.com/ten.)

be divided into the proliferation, differentiation, and mineralization stages,[47] and the effects of a pulsed electromagnetic field depend on the maturation stages of the osteoblasts.[18] The increase in bone formation depends on the increase in extracellular matrix synthesis,[48] and the type I collagen synthesis is upregulated at the proliferation stage, when the osteoblasts are not confluent, and downregulated at the subsequent stages.[47,49] Aaron and Ciombor reported a significant increase in extracellular matrix synthesis when the osteoblast-like cells were subjected to an electromagnetic stimulation.[50] Heermeier *et al.* showed the electromagnetic upregulation of type I collagen and the TGF-β potential in terms of mitosis and differentiation.[14] In this study, the mature SAOS-2 osteoblasts were in the

Table 1. Amount of Extracellular Matrix Constituents over the Scaffold Surface After the Whole Culture Period: The Electromagnetic Stimulation Increased Protein Amount

	Matrix protein coating after 22 days of culture in fg/(cell×scaffold)		
	Static culture	*Dynamic culture*	*Dynamic/static*
Decorin	94.55 ± 2.43	124.13 ± 12.53	1.3-fold
Osteocalcin	82.65 ± 12.16	1012.70 ± 27.63	12.2-fold
Osteopontin	249.77 ± 2.03	3029.40 ± 163.84	12.1-fold
Type I collagen	969.08 ± 186.13	9722.20 ± 408.40	10.0-fold
Type III collagen	409.33 ± 8.81	4307.10 ± 180.70	10.5-fold

($p < 0.05$ for each protein)

proliferation stage on the surface of 3D porous polyurethane scaffolds. According to preceding studies, the electromagnetic bioreactor caused a significant increase in extracellular matrix synthesis: in comparison with static culture, the surface deposition of type I collagen was approximately 10 times as great, and the whole secretion in the culture medium was approximately 1.6 times as great. Type I collagen is the most important and abundant structural protein of bone matrix, and decorin is an important proteoglycan considered to be a key regulator for the assembly and function of many extracellular matrix proteins. Decorin plays a major role in the lateral growth of collagen fibrils; in comparison, the incorporation of decorin inside the matrix was approximately 1.3 times greater than with control culture, whereas the whole secretion in the culture medium was approximately 1.9 times greater. The immunolocalization of type I collagen and decorin showed their colocalization in the cell-rich areas. The secretions of these proteins in the culture medium showed an exponentially decreasing temporal pattern, and the asymptotic growth model best fitted the total secretions, with $R^2 > 0.99$, indicating that, after 22 days of culture, the completion of the matrix deposition was approaching inside the electromagnetic bioreactor. Heermeier *et al.* observed a similar localization of type I collagen in the cell-rich areas and a concordant decrease in type I collagen messenger RNA levels after 21 days of culture.[14]

Other fundamental matrix constituents are type III collagen, osteopontin, and osteocalcin. Osteopontin is a glycosylated bone phosphoprotein secreted during the early stages of osteogenesis; before the onset of mineralization, it binds calcium, and it is probably involved in the regulation of hydroxyapatite crystal growth, whereas osteocalcin is secreted after the onset of mineralization, and it binds to bone minerals. The surface deposition of type III collagen, osteopontin, and osteocalcin was approximately $10 \div 12$ times as great as with static culture, and the whole secretion in the culture medium approximately $1.1 \div 1.5$ times as great. The immunolocalization of these matrix proteins showed their colocalization in the cell-rich areas, such as type I collagen and decorin. Considering the role of osteopontin and osteocalcin in the matrix calcification process, and considering the delay of the osteocalcin expression peak in the static culture, we observed a concordant 5 times as great matrix calcification inside the electromagnetic bioreactor; moreover, the calcification was localized in the cell-rich areas, like the studied matrix constituents; in other words, calcium and matrix proteins were colocalized.

The increase in mineralization was consistent with the rise in alkaline phosphatase expression in response to an electromagnetic wave exposure, as reported in other studies.[51,52] Alkaline phosphatase plays an important role in the matrix mineralization process, it binds calcium phosphates, and it hydrolyzes the phosphate sources. In this study, we used 10 mM β-glycerophosphate as a source of phosphates. Some researchers have shown that, in static culture systems, such a high concentration could give rise to non-apatitic calcium phosphate phases;[53,54] another static culture study reported that, in a chick osteogenesis model, cultures supplemented

Table 2. Total Secretion of Extracellular Matrix Constituents in the Culture Medium After the Whole Culture Period: The Electromagnetic Stimulation Increased Protein Total Secretion

	Matrix protein total secretion after 22 days of culture in fg/(cell×scaffold)		
	Static culture	*Dynamic culture*	*Dynamic/static*
Decorin	0.98 ± 0.12	1.94 ± 0.22	1.9-fold
Osteocalcin	3.22 ± 0.35	4.75 ± 0.37	1.5-fold
Osteopontin	54.83 ± 1.43	60.76 ± 1.03	1.1-fold
Type I collagen	151.80 ± 10.54	246.65 ± 16.71	1.6-fold
Type III collagen	42.38 ± 4.17	64.13 ± 7.65	1.5-fold

($p < 0.05$ for each protein)

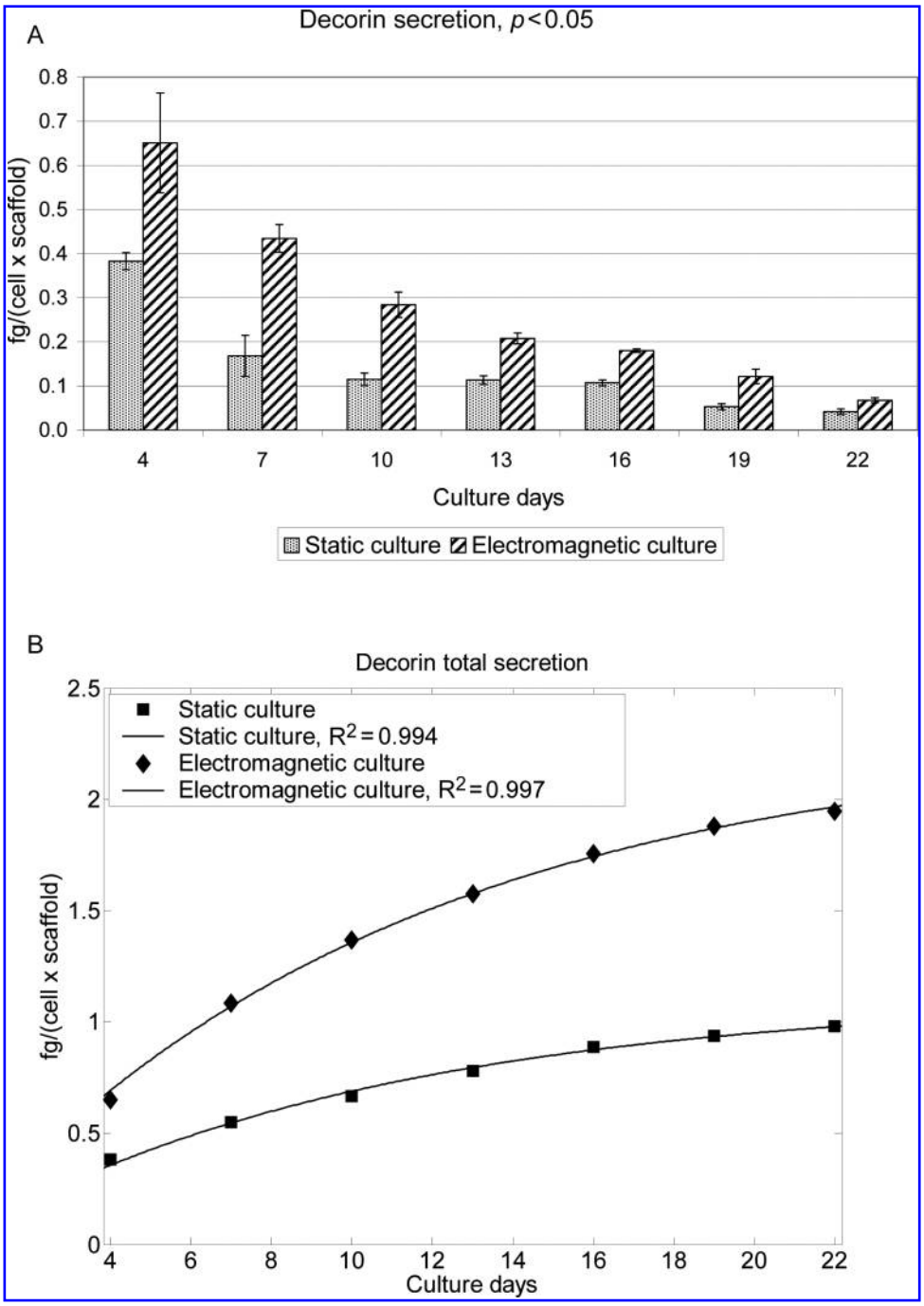

FIG. 7. Decorin secretion at each medium change (**A**) and total secretion (**B**). At each medium change, the electromagnetic stimulation increased decorin synthesis ($p < 0.05$).

with inorganic phosphate failed to mineralize, whereas those with 10 mM β-glycerophosphate mineralized.[55] Farley *et al.* showed that, in a SAOS-2 cell model, the specific activity of alkaline phosphatase was proportional to phosphate concentration.[56] In the tissue-engineering field, a high concentration of β-glycerophosphate, a substrate for alkaline phosphatase, appears justified whenever the culture method (e.g., shear stress stimulation[8] and electromagnetic wave exposure[51,52]) could cause a significant rise in alkaline phosphatase activity; for instance, Bancroft *et al.*[8] stimulated marrow stromal osteoblasts using fluid flow perfusion, obtaining a great increase in alkaline phosphatase activity and in matrix mineralization.

The electromagnetic stimulation raises the net Ca^{2+} flux in human osteoblast-like cells,[57] and, according to Pavalko's diffusion-controlled/solid-state signaling model,[58] the increase in the cytosolic Ca^{2+} concentration is the starting point of signaling pathways targeting specific bone

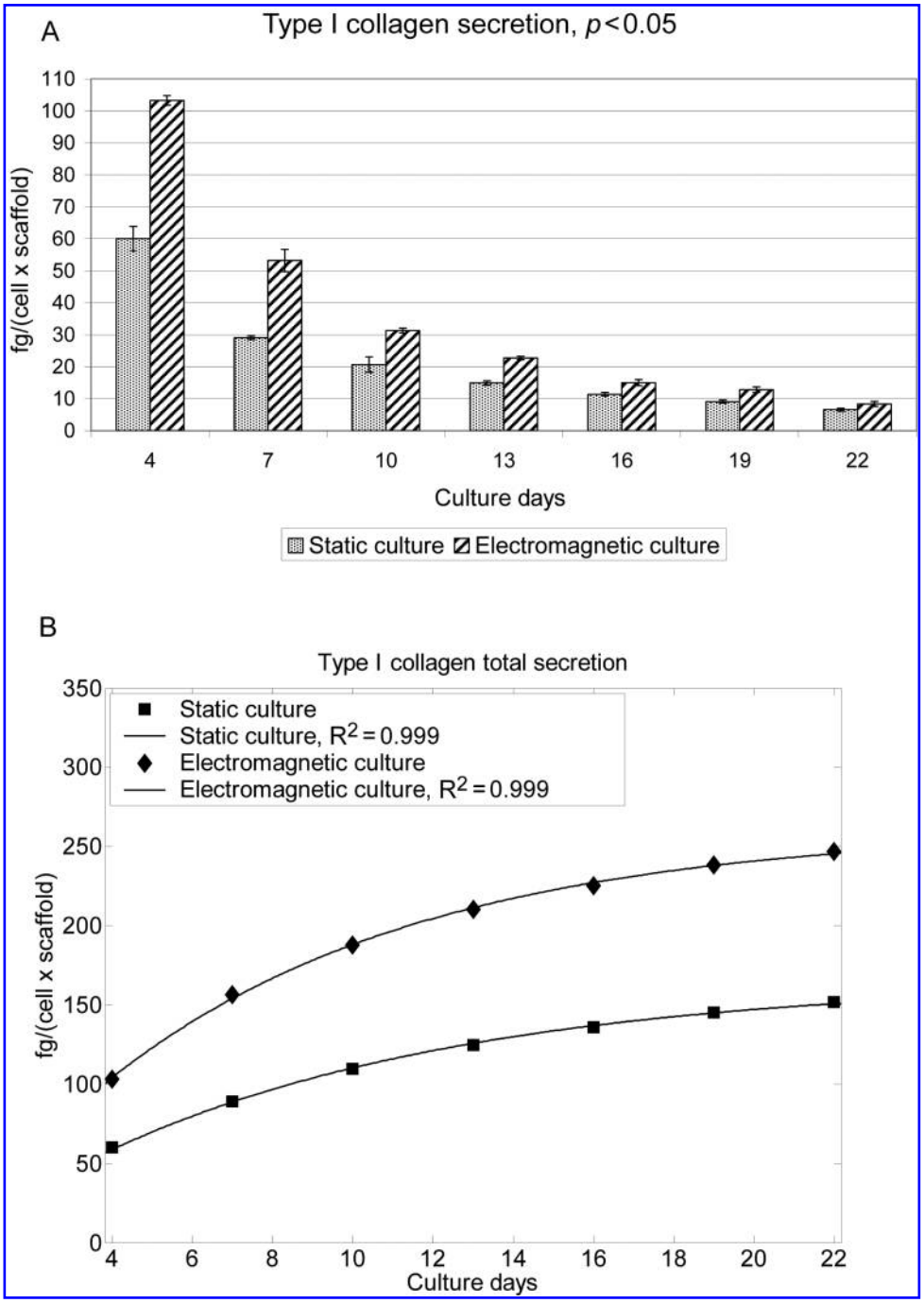

FIG. 8. Type I collagen secretion at each medium change (**A**) and total secretion (**B**). At each medium change, the electromagnetic stimulation increased type I collagen synthesis ($p < 0.05$).

matrix genes. Considering Pavalko's model, the analysis of the transcripts specific for decorin, fibronectin, osteocalcin, osteopontin, TGF-β, type I collagen, and type III collagen revealed, concordantly, that the application of the electromagnetic wave caused greater gene transcription than with static culture. Fibronectin and TGF-β were studied using only the RT-PCR method because contaminations due to culture medium serum are possible.

In this study, using an electromagnetic stimulation, we enhanced a SAOS-2 cell culture over a porous polyurethane suitable for bone-tissue engineering.

The choice of the cell line was justified. An ability to induce the formation of new bone at a specific site would represent a significant advance in bone repair and tissue engineering. This property seems to belong to SAOS-2 cells. These osteoblasts contain a unique osteoinductive activity,

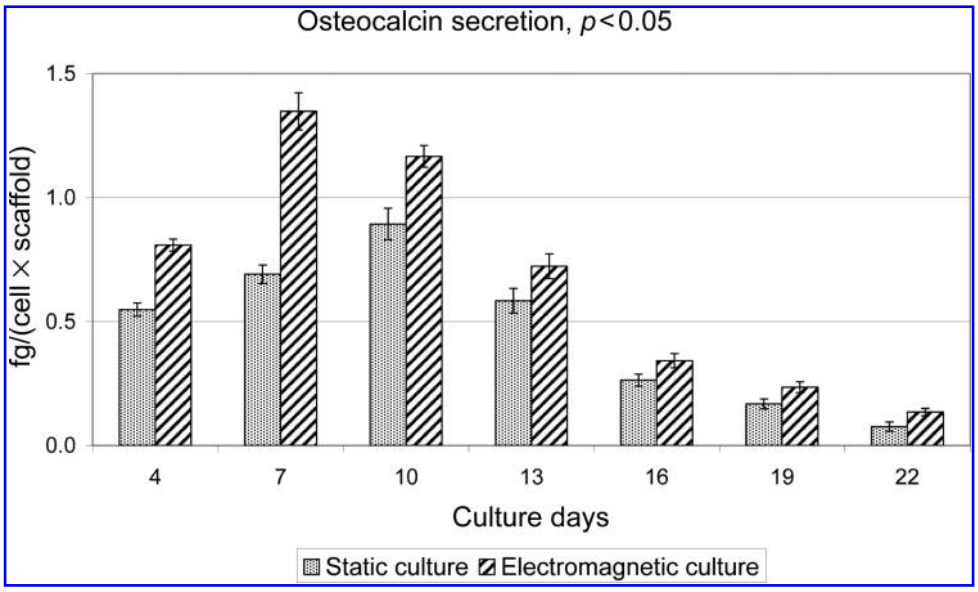

FIG. 9. Osteocalcin secretion at each medium change. At each medium change, the electromagnetic stimulation increased osteocalcin synthesis ($p < 0.05$).

whereas other human osteosarcoma cells, such as U-2 OS, cannot replicate that bone-inducing ability.[28] Devitalized SAOS-2 cells, extracts, and secretions induced the formation of new bone when implanted subcutaneously in *nu/nu* mice.[59,60] These osteoblasts can be grown, virtually indefinitely, to produce large quantities of osteoinductive factors, such as bone sialoprotein and osteonectin.[28]

The choice of the biomaterial was also justified. Gorna and Gogolewski[6,23] designed biodegradable crosslinked polyurethanes suitable for bone repair in terms of pore size, porosity, and mechanical properties; the mechanical properties of such substitutes are of minor importance, because metallic internal fixation devices may ensure the mechanical stability of the bone-scaffold system.[6] Our polyurethane was similar in terms of pore size, porosity, and mechanical properties. Nevertheless, it was non-biodegradable, owing to its chemical structure and hydrophobia.[10] The use of this polyurethane foam would overcome the possible problems associated with the biodegradable polymers, such as degradation kinetics asynchronous with tissue regeneration and adverse reactions to degradation products.

In this study, we demonstrated that the polyurethane scaffolds can be suitable to calcified matrix coating under electromagnetic stimulation, making the biomaterial useful for biointegration (i.e., the *in vivo* integration of a biostable biomaterial).[10] We have reported that, inside the electromagnetic bioreactor, the coating with matrix constituents was greatly enhanced. We could suppose that the seeded osteoblasts adhered to the hydrophobic polyurethane through serum-adsorbed proteins[61,62] and that they then adhered to secreted matrix proteins, especially type I collagen. The electromagnetic stimulation made more adhesion proteins available; in other words, it permitted more efficient development of the biomaterial-matrix-cell system.

In conclusion, calcified matrix-coated scaffolds could be used in clinical applications as osteoinductive agents for bone repair. Nevertheless, a better result could be obtained with bone marrow stromal osteoblasts instead of SAOS-2 cells for total immunocompatibility with the patient.

ACKNOWLEDGMENTS

The authors thank Prof. L.W. Fisher, Prof. P. Speziale, Prof. A. Casasco, Prof. A. Icaro-Cornaglia, Prof. F. Auricchio, Prof. G. Parravicini, Dr. S. Setti, Dr. R. Cadossi, Dr. C. Giudici, Dr. S. Farè, Dr. P. Petrini, Mr. D. Picenoni, and Mr. A. Mortara for support. The Biostim SPT pulse generator was a gift from Igea (Carpi, Italy). This work was supported by Fondazione Cariplo Grant (2004) to Prof. F. Benazzo; a PRIN Grant (2004) from the Italian Ministry of Education, University and Research to Dr. L. Visai; and FAR Grants (2004) from the University of Pavia to Prof. F. Benazzo, Prof. M.G. Cusella De Angelis, and Prof. G. Magenes.

REFERENCES

1. Nishikawa, M., Myoui, A., Ohgushi, H., Ikeuchi, M., Tamai, N., and Yoshikawa, H. Bone tissue engineering using novel interconnected porous hydroxyapatite ceramics combined with marrow mesenchymal cells: quantitative and three-dimensional image analysis. Cell Transplant. **13,** 367, 2004.
2. Mauney, J.R., Blumberg, J., Pirun, M., Volloch, V., Vunjak-Novakovic, G., and Kaplan, D.L. Osteogenic differentiation of human bone marrow stromal cells on partially demineralized bone scaffolds in vitro. Tissue Eng. **10,** 81, 2004.

3. Ishaug-Riley, S.L., Crane, G.M., Gurlek, A., Miller, M.J., Yasko, A.W., Yaszemski, M.J., and Mikos, A.G. Ectopic bone formation by marrow stromal osteoblast transplantation using poly(DL-lactic-co-glycolic acid) foams implanted into the rat mesentery. J. Biomed. Mater. Res. **36,** 1, 1997.
4. Devin, J.E., Attawia, M.A., and Laurencin, C.T. Three-dimensional degradable porous polymer-ceramic matrices for use in bone repair. J. Biomater. Sci. Polym. Ed. **7,** 661, 1996.
5. Gomes, M.E., Sikavitsas, V.I., Behravesh, E., Reis, R.L., and Mikos, A.G. Effect of flow perfusion on the osteogenic differentiation of bone marrow stromal cells cultured on starch-based three-dimensional scaffolds. J. Biomed. Mater. Res. **A 67,** 87, 2003.
6. Gorna, K., and Gogolewski, S. Preparation, degradation, and calcification of biodegradable polyurethane foams for bone graft substitutes. J. Biomed. Mater. Res. **A 67,** 813, 2003.
7. Botchwey, E.A., Pollack, S.R., Levine, E.M., and Laurencin, C.T. Bone tissue engineering in a rotating bioreactor using a microcarrier matrix system. J. Biomed. Mater. Res. **55,** 242, 2001.
8. Bancroft, G.N., Sikavitsas, V.I., van den Dolder, J., Sheffield, T.L., Ambrose, C.G., Jansen, J.A., and Mikos, A.G. Fluid flow increases mineralized matrix deposition in 3D perfusion culture of marrow stromal osteoblasts in a dose-dependent manner. Proc. Natl. Acad. Sci. U.S.A. **99,** 12600, 2002.
9. Akita, S., Tamai, N., Myoui, A., Nishikawa, M., Kaito, T., Takaoka, K., and Yoshikawa, H. Capillary vessel network integration by inserting a vascular pedicle enhances bone formation in tissue-engineered bone using interconnected porous hydroxyapatite ceramics. Tissue Eng. **10,** 789, 2004.
10. Fassina, L., Visai, L., Asti, L., Benazzo, F., Speziale, P., Tanzi, M.C., and Magenes, G. Calcified matrix production by SAOS-2 cells inside a polyurethane porous scaffold, using a perfusion bioreactor. Tissue Eng. **11,** 685, 2005.
11. Ciombor, D.M., and Aaron, R.K. Influence of electromagnetic fields on endochondral bone formation. J. Cell. Biochem. **52,** 37, 1993.
12. Matsunaga, S., Sakou, T., and Ijiri, K. Osteogenesis by pulsing electromagnetic fields (PEMFs): optimum stimulation setting. In Vivo **10,** 351, 1996.
13. Otter, M.W., McLeod, K.J., and Rubin, C.T. Effects of electromagnetic fields in experimental fracture repair. Clin. Orthop. Relat. Res. **355S,** S90, 1998.
14. Heermeier, K., Spanner, M., Trager, J., Gradinger, R., Strauss, P.G., Kraus, W., and Schmidt, J. Effects of extremely low frequency electromagnetic field (EMF) on collagen type I mRNA expression and extracellular matrix synthesis of human osteoblastic cells. Bioelectromagnetics **19,** 222, 1998.
15. De Mattei, M., Caruso, A., Traina, G.C., Pezzetti, F., Baroni, T., and Sollazzo, V. Correlation between pulsed electromagnetic fields exposure time and cell proliferation increase in human osteosarcoma cell lines and human normal osteoblast cells in vitro. Bioelectromagnetics **20,** 177, 1999.
16. Lohmann, C.H., Schwartz, Z., Liu, Y., Guerkov, H., Dean, D.D., Simon, B., and Boyan, B.D. Pulsed electromagnetic field stimulation of MG63 osteoblast-like cells affects differentiation and local factor production. J. Orthop. Res. **18,** 637, 2000.
17. Guerkov, H.H., Lohmann, C.H., Liu, Y., Dean, D.D., Simon, B.J., Heckman, J.D., Schwartz, Z., and Boyan, B.D. Pulsed electromagnetic fields increase growth factor release by nonunion cells. Clin. Orthop. Relat. Res. **384,** 265, 2001.
18. Diniz, P., Shomura, K., Soejima, K., and Ito, G. Effects of pulsed electromagnetic field (PEMF) stimulation on bone tissue like formation are dependent on the maturation stages of the osteoblasts. Bioelectromagnetics **23,** 398, 2002.
19. Lohmann, C.H., Schwartz, Z., Liu, Y., Li, Z., Simon, B.J., Sylvia, V.L., Dean, D.D., Bonewald, L.F., Donahue, H.J., and Boyan, B.D. Pulsed electromagnetic fields affect phenotype and connexin 43 protein expression in MLO-Y4 osteocyte-like cells and ROS 17/2.8 osteoblast-like cells. J. Orthop. Res. **21,** 326, 2003.
20. Aaron, R.K., Ciombor, D.M., and Simon, B.J. Treatment of nonunions with electric and electromagnetic fields. Clin. Orthop. Relat. Res. **419,** 21, 2004.
21. Aaron, R.K., Boyan, B.D., Ciombor, D.M., Schwartz, Z., and Simon, B.J. Stimulation of growth factor synthesis by electric and electromagnetic fields. Clin. Orthop. Relat. Res. **419,** 30, 2004.
22. Chang, W.H., Chen, L.T., Sun, J.S., and Lin, F.H. Effect of pulse-burst electromagnetic field stimulation on osteoblast cell activities. Bioelectromagnetics **25,** 457, 2004.
23. Gorna, K., and Gogolewski, S. Biodegradable polyurethanes for implants. II. In vitro degradation and calcification of materials from poly(epsilon-caprolactone)-poly(ethylene oxide) diols and various chain extenders. J. Biomed. Mater. Res. **60,** 592, 2002.
24. Vert, M., Mauduit, J., and Li, S. Biodegradation of PLA/GA polymers: increasing complexity. Biomaterials **15,** 1209, 1994.
25. Bobyn, J.D., Stackpool, G.J., Hacking, S.A., Tanzer, M., and Krygier, J.J. Characteristics of bone ingrowth and interface mechanics of a new porous tantalum biomaterial. J. Bone Joint Surg. Br. **81,** 907, 1999.
26. Zou, X., Li, H., Baatrup, A., Lind, M., and Bunger, C. Engineering of bone tissue with porcine bone marrow stem cells in three-dimensional trabecular metal: in vitro and in vivo studies. APMIS Suppl. **109,** 127, 2003.
27. van den Dolder, J., Farber, E., Spauwen, P.H., and Jansen, J.A. Bone tissue reconstruction using titanium fiber mesh combined with rat bone marrow stromal cells. Biomaterials **24,** 1745, 2003.
28. Anderson, H.C., Reynolds, P.R., Hsu, H.H., Missana, L., Masuhara, K., Moylan, P.E., and Roach, H.I. Selective synthesis of bone morphogenetic proteins-1, -3, -4 and bone sialoprotein may be important for osteoinduction by Saos-2 cells. J. Bone Miner. Metab. **20,** 73, 2002.
29. Belanger, M.C., Marois, Y., Roy, R., Mehri, Y., Wagner, E., Zhang, Z., King, M.W., Yang, M., Hahn, C., and Guidoin, R. Selection of a polyurethane membrane for the manufacture of ventricles for a totally implantable artificial heart: blood compatibility and biocompatibility studies. Artif. Organs **24,** 879, 2000.
30. Banerjee, A.G., Bhattacharyya, I., Lydiatt, W.M., and Vishwanatha, J.K. Aberrant expression and localization of decorin in human oral dysplasia and squamous cell carcinoma. Cancer Res. **63,** 7769, 2003.
31. Liang, X., Zhang, H., Zhou, A., and Wang, H. AngRem104, an angiotensin II-induced novel upregulated gene in human mesangial cells, is potentially involved in the regulation of fibronectin expression. J. Am. Soc. Nephrol. **14,** 1443, 2003.
32. Yamada, Y., Ando, F., Niino, N., and Shimokata, H. Association of polymorphisms of interleukin-6, osteocalcin, and vitamin D receptor genes, alone or in combination, with bone mineral density in community-dwelling Japanese women and men. J. Clin. Endocrinol. Metab. **88,** 3372, 2003.

33. Iwata, M., Awaya, N., Graf, L., Kahl, C., and Torok-Storb, B. Human marrow stromal cells activate monocytes to secrete osteopontin, which down-regulates Notch1 gene expression in CD34+ cells. Blood **103,** 4496, 2004.
34. Derynck, R., Jarrett, J.A., Chen, E.Y., Eaton, D.H., Bell, J.R., Assoian, R.K., Roberts, A.B., Sporn, M.B., and Goeddel, D.V. Human transforming growth factor-beta complementary DNA sequence and expression in normal and transformed cells. Nature **316,** 701, 1985.
35. Makela, J.K., Vuorio, T., and Vuorio, E. Growth-dependent modulation of type I collagen production and mRNA levels in cultured human skin fibroblasts. Biochim. Biophys. Acta **1049,** 171, 1990.
36. Fu, S.C., Wong, Y.P., Cheuk, Y.C., Lee, K.M., and Chan, K.M. TGF-beta1 reverses the effects of matrix anchorage on the gene expression of decorin and procollagen type I in tendon fibroblasts. Clin. Orthop. Relat. Res. **431,** 226, 2005.
37. Overbergh, L., Valckx, D., Waer, M., and Mathieu, C. Quantification of murine cytokine mRNAs using real time quantitative reverse transcriptase PCR. Cytokine **11,** 305, 1999.
38. Fisher, L.W., Termine, J.D., and Young, M.F. Deduced protein sequence of bone small proteoglycan I (biglycan) shows homology with proteoglycan II (decorin) and several nonconnective tissue proteins in a variety of species. J. Biol. Chem. **264,** 4571, 1989.
39. Bianco, P., Fisher, L.W., Young, M.F., Termine, J.D., and Robey, P.G. Expression and localization of the two small proteoglycans biglycan and decorin in developing human skeletal and nonskeletal tissues. J. Histochem. Cytochem. **38,** 1549, 1990.
40. Fisher, L.W., Stubbs, J.T., III, and Young, M.F. Antisera and cDNA probes to human and certain animal model bone matrix noncollagenous proteins. Acta Orthop. Scand. Suppl. **266,** 61, 1995.
41. Vogel, K.G., and Evanko, S.P. Proteoglycans of fetal bovine tendon. J. Biol. Chem. **262,** 13607, 1987.
42. Rossi, A., Zuccarello, L.V., Zanaboni, G., Monzani, E., Dyne, K.M., Cetta, G., and Tenni, R. Type I collagen CNBr peptides: species and behavior in solution. Biochemistry **35,** 6048, 1996.
43. Hsu, S.M., Raine, L., and Fanger, H. The use of antiavidin antibody and avidin-biotin-peroxidase complex in immunoperoxidase technics. Am. J. Clin. Pathol. **75,** 816, 1981.
44. Cane, V., Botti, P., and Soana, S. Pulsed magnetic fields improve osteoblast activity during the repair of an experimental osseous defect. J. Orthop. Res. **11,** 664, 1993.
45. Bodamyali, T., Bhatt, B., Hughes, F.J., Winrow, V.R., Kanczler, J.M., Simon, B., Abbott, J., Blake, D.R., and Stevens, C.R. Pulsed electromagnetic fields simultaneously induce osteogenesis and upregulate transcription of bone morphogenetic proteins 2 and 4 in rat osteoblasts in vitro. Biochem. Biophys. Res. Commun. **250,** 458, 1998.
46. Fitzsimmons, R.J., Ryaby, J.T., Magee, F.P., and Baylink, D.J. IGF-II receptor number is increased in TE-85 osteosarcoma cells by combined magnetic fields. J. Bone Miner. Res. **10,** 812, 1995.
47. Owen, T.A., Aronow, M., Shalhoub, V., Barone, L.M., Wilming, L., Tassinari, M.S., Kennedy, M.B., Pockwinse, S., Lian, J.B., and Stein, G.S. Progressive development of the rat osteoblast phenotype in vitro: reciprocal relationships in expression of genes associated with osteoblast proliferation and differentiation during formation of the bone extracellular matrix. J. Cell. Physiol. **143,** 420, 1990.
48. Manolagas, S.C. Birth and death of bone cells: basic regulatory mechanisms and implications for the pathogenesis and treatment of osteoporosis. Endocr. Rev. **21,** 115, 2000.
49. Quarles, L.D., Yohay, D.A., Lever, L.W., Caton, R., and Wenstrup, R.J. Distinct proliferative and differentiated stages of murine MC3T3-E1 cells in culture: an in vitro model of osteoblast development. J. Bone Miner. Res. **7,** 683, 1992.
50. Aaron, R.K., and Ciombor, D.M. Acceleration of experimental endochondral ossification by biophysical stimulation of the progenitor cell pool. J. Orthop. Res. **14,** 582, 1996.
51. Sert, C., Mustafa, D., Duz, M.Z., Aksen, F., and Kaya, A. The preventive effect on bone loss of 50-Hz, 1-mT electromagnetic field in ovariectomized rats. J. Bone Miner. Metab. **20,** 345, 2002.
52. Torricelli, P., Fini, M., Giavaresi, G., Botter, R., Beruto, D., and Giardino, R. Biomimetic PMMA-based bone substitutes: a comparative in vitro evaluation of the effects of pulsed electromagnetic field exposure. J. Biomed. Mater. Res. **A 64,** 182, 2003.
53. Chung, C.H., Golub, E.E., Forbes, E., Tokuoka, T., and Shapiro, I.M. Mechanism of action of beta-glycerophosphate on bone cell mineralization. Calcif. Tissue Int. **51,** 305, 1992.
54. Davies, J.E. In vitro modeling of the bone/implant interface. Anat. Rec. **245,** 426, 1996.
55. Tenenbaum, H.C., McCulloch, C.A., Fair, C., and Birek, C. The regulatory effect of phosphates on bone metabolism in vitro. Cell Tissue Res. **257,** 555, 1989.
56. Farley, J.R., Hall, S.L., Tanner, M.A., and Wergedal, J.E. Specific activity of skeletal alkaline phosphatase in human osteoblast-line cells regulated by phosphate, phosphate esters, and phosphate analogs and release of alkaline phosphatase activity inversely regulated by calcium. J. Bone Miner. Res. **9,** 497, 1994.
57. Fitzsimmons, R.J., Ryaby, J.T., Magee, F.P., and Baylink, D.J. Combined magnetic fields increased net calcium flux in bone cells. Calcif. Tissue Int. **55,** 376, 1994.
58. Pavalko, F.M., Norvell, S.M., Burr, D.B., Turner, C.H., Duncan, R.L., and Bidwell, J.P. A model for mechanotransduction in bone cells: the load-bearing mechanosomes. J. Cell. Biochem. **88,** 104, 2003.
59. Anderson, H.C., Sugamoto, K., Morris, D.C., Hsu, H.H., and Hunt, T. Bone-inducing agent (BIA) from cultured human Saos-2 osteosarcoma cells. Bone Miner. **16,** 49, 1992.
60. Anderson, H.C., Hsu, H.H., Raval, P., Hunt, T.R., Schwappach, J.R., Morris, D.C., and Schneider, D.J. The mechanism of bone induction and bone healing by human osteosarcoma cell extracts. Clin. Orthop. Relat. Res. 129, 1995.
61. El-Ghannam, A., Ducheyne, P., and Shapiro, I.M. Effect of serum proteins on osteoblast adhesion to surface-modified bioactive glass and hydroxyapatite. J. Orthop. Res. **17,** 340, 1999.
62. Yang, Y., Cavin, R., and Ong, J.L. Protein adsorption on titanium surfaces and their effect on osteoblast attachment. J. Biomed. Mater. Res. **A 67,** 344, 2003.

Address reprint requests to:
Lorenzo Fassina, M.Sc.
Università di Pavia
Dipartimento di Informatica e Sistemistica
via Ferrata, 1
27100 Pavia, Italy

E-mail: lorenzo.fassina@unipv.it

This article has been cited by:

1. P. C. Grunert, A. Jonitz-Heincke, Y. Su, R. Souffrant, D. Hansmann, H. Ewald, A. Krüger, W. Mittelmeier, R. Bader. 2014. Establishment of a Novel In Vitro Test Setup for Electric and Magnetic Stimulation of Human Osteoblasts. *Cell Biochemistry and Biophysics* **70**, 805-817. [CrossRef]
2. T. Saliev, Z. Mustapova, G. Kulsharova, D. Bulanin, S. Mikhalovsky. 2014. Therapeutic potential of electromagnetic fields for tissue engineering and wound healing. *Cell Proliferation* n/a-n/a. [CrossRef]
3. GyuHyun Jin, Gi-Hoon Yang, GeunHyung Kim. 2014. Tissue engineering bioreactor systems for applying physical and electrical stimulations to cells. *Journal of Biomedical Materials Research Part B: Applied Biomaterials* n/a-n/a. [CrossRef]
4. L. de Girolamo, M. Viganò, E. Galliera, D. Stanco, S. Setti, M. G. Marazzi, G. Thiebat, M. M. Corsi Romanelli, V. Sansone. 2014. In vitro functional response of human tendon cells to different dosages of low-frequency pulsed electromagnetic field. *Knee Surgery, Sports Traumatology, Arthroscopy* . [CrossRef]
5. Jung Min Hong, Kyung Shin Kang, Hee-Gyeong Yi, Shin-Yoon Kim, Dong-Woo Cho. 2014. Electromagnetically controllable osteoclast activity. *Bone* **62**, 99-107. [CrossRef]
6. Ji-zhe Yu, Hua Wu, Yong Yang, Chao-xu Liu, Yang Liu, Ming-yu Song. 2014. Osteogenic differentiation of bone mesenchymal stem cells regulated by osteoblasts under EMF exposure in a co-culture system. *Journal of Huazhong University of Science and Technology [Medical Sciences]* **34**, 247-253. [CrossRef]
7. Nicoletta Marchesi, Cecilia Osera, Lorenzo Fassina, Marialaura Amadio, Francesca Angeletti, Martina Morini, Giovanni Magenes, Letizia Venturini, Marco Biggiogera, Giovanni Ricevuti, Stefano Govoni, Salvatore Caorsi, Alessia Pascale, Sergio Comincini. 2014. Autophagy Is Modulated in Human Neuroblastoma Cells Through Direct Exposition to Low Frequency Electromagnetic Fields. *Journal of Cellular Physiology* n/a-n/a. [CrossRef]
8. L. Fassina, P. Dubruel, G. Magenes, S. Van VlierberghePotential of electromagnetic and ultrasound stimulations for bone regeneration 445-459. [CrossRef]
9. Maria Mognaschi, Paolo Di Barba, Giovanni Magenes, Andrea Lenzi, Fabio Naro, Lorenzo Fassina. 2014. Field models and numerical dosimetry inside an extremely-low-frequency electromagnetic bioreactor: the theoretical link between the electromagnetically induced mechanical forces and the biological mechanisms of the cell tensegrity. *SpringerPlus* **3**, 473. [CrossRef]
10. Marie Hronik-Tupaj, Waseem Khan Raja, Min Tang-Schomer, Fiorenzo G. Omenetto, David L. Kaplan. 2013. Neural responses to electrical stimulation on patterned silk films. *Journal of Biomedical Materials Research Part A* **101A**:10.1002/jbm.a.v101a.9, 2559-2572. [CrossRef]
11. L. Girolamo, D. Stanco, E. Galliera, M. Viganò, A. Colombini, S. Setti, E. Vianello, M. M. Corsi Romanelli, V. Sansone. 2013. Low Frequency Pulsed Electromagnetic Field Affects Proliferation, Tissue-Specific Gene Expression, and Cytokines Release of Human Tendon Cells. *Cell Biochemistry and Biophysics* . [CrossRef]
12. D. Prè, G. Ceccarelli, L. Visai, L. Benedetti, M. Imbriani, M. G. Cusella De Angelis, G. Magenes. 2013. High-Frequency Vibration Treatment of Human Bone Marrow Stromal Cells Increases Differentiation toward Bone Tissue. *Bone Marrow Research* **2013**, 1-13. [CrossRef]
13. Kyung Shin Kang, Jung Min Hong, Jo A Kang, Jong-Won Rhie, Young Hun Jeong, Dong-Woo Cho. 2013. Regulation of osteogenic differentiation of human adipose-derived stem cells by controlling electromagnetic field conditions. *Experimental & Molecular Medicine* **45**, e6. [CrossRef]
14. GyuHyun Jin, GeunHyung Kim. 2013. The effect of sinusoidal AC electric stimulation of 3D PCL/CNT and PCL/β-TCP based bio-composites on cellular activities for bone tissue regeneration. *Journal of Materials Chemistry B* **1**, 1439. [CrossRef]
15. Richard A. Thibault, Antonios G. Mikos, F. Kurtis Kasper. 2013. Scaffold/Extracellular Matrix Hybrid Constructs for Bone-Tissue Engineering. *Advanced Healthcare Materials* **2**:10.1002/adhm.v2.1, 13-24. [CrossRef]
16. Kyung Shin Kang, Jung Min Hong, Young-Joon Seol, Jong-Won Rhie, Young Hun Jeong, Dong-Woo Cho. 2012. Short-term evaluation of electromagnetic field pretreatment of adipose-derived stem cells to improve bone healing. *Journal of Tissue Engineering and Regenerative Medicine* n/a-n/a. [CrossRef]
17. Marie Hronik-Tupaj, David L. Kaplan. 2012. A Review of the Responses of Two- and Three-Dimensional Engineered Tissues to Electric Fields. *Tissue Engineering Part B: Reviews* **18**:3, 167-180. [Abstract] [Full Text HTML] [Full Text PDF] [Full Text PDF with Links]
18. D.J. Mooney, D. ShvartsmanProgramming Cells with Synthetic Polymers 485-495. [CrossRef]
19. Yu Zhang, Dilaware Khan, Julia Delling, Edda Tobiasch. 2012. Mechanisms Underlying the Osteo- and Adipo-Differentiation of Human Mesenchymal Stem Cells. *The Scientific World Journal* **2012**, 1-14. [CrossRef]

20. Cecilia Osera, Lorenzo Fassina, Marialaura Amadio, Letizia Venturini, Erica Buoso, Giovanni Magenes, Stefano Govoni, Giovanni Ricevuti, Alessia Pascale. 2011. Cytoprotective Response Induced by Electromagnetic Stimulation on SH-SY5Y Human Neuroblastoma Cell Line. *Tissue Engineering Part A* **17**:19-20, 2573-2582. [Abstract] [Full Text HTML] [Full Text PDF] [Full Text PDF with Links]
21. Juliane Rauh, Falk Milan, Klaus-Peter Günther, Maik Stiehler. 2011. Bioreactor Systems for Bone Tissue Engineering. *Tissue Engineering Part B: Reviews* **17**:4, 263-280. [Abstract] [Full Text HTML] [Full Text PDF] [Full Text PDF with Links]
22. D. Prè, G. Ceccarelli, G. Gastaldi, A. Asti, E. Saino, L. Visai, F. Benazzo, M.G. Cusella De Angelis, G. Magenes. 2011. The differentiation of human adipose-derived stem cells (hASCs) into osteoblasts is promoted by low amplitude, high frequency vibration treatment. *Bone* **49**, 295-303. [CrossRef]
23. Alessia Ongaro, Agnese Pellati, Federica Francesca Masieri, Angelo Caruso, Stefania Setti, Ruggero Cadossi, Roberto Biscione, Leo Massari, Milena Fini, Monica De Mattei. 2011. Chondroprotective effects of pulsed electromagnetic fields on human cartilage explants. *Bioelectromagnetics* n/a-n/a. [CrossRef]
24. Hsin-Yi Lin, Yu-Jen Lin. 2011. In vitro effects of low frequency electromagnetic fields on osteoblast proliferation and maturation in an inflammatory environment. *Bioelectromagnetics* n/a-n/a. [CrossRef]
25. Vincenzo Sollazzo, Annalisa Palmieri, Furio Pezzetti, Leo Massari, Francesco Carinci. 2010. Effects of Pulsed Electromagnetic Fields on Human Osteoblastlike Cells (MG-63): A Pilot Study. *Clinical Orthopaedics and Related Research®* **468**, 2260-2277. [CrossRef]
26. Sheng-Wei Feng, Yi-June Lo, Wei-Jen Chang, Che-Tong Lin, Sheng-Yang Lee, Yoshimitsu Abiko, Haw-Ming Huang. 2010. Static magnetic field exposure promotes differentiation of osteoblastic cells grown on the surface of a poly-l-lactide substrate. *Medical & Biological Engineering & Computing* **48**, 793-798. [CrossRef]
27. Piotr Woźniak, Monika Bil, Joanna Ryszkowska, Piotr Wychowański, Edyta Wróbel, Anna Ratajska, Grażyna Hoser, Jacek Przybylski, Krzysztof J. Kurzydłowski, Małgorzata Lewandowska-Szumieł. 2010. Candidate bone-tissue-engineered product based on human-bone-derived cells and polyurethane scaffold. *Acta Biomaterialia* **6**, 2484-2493. [CrossRef]
28. Enrica Saino, Valentina Maliardi, Eliana Quartarone, Lorenzo Fassina, Laura Benedetti, Maria Gabriella Cusella De Angelis, Piercarlo Mustarelli, Alessandro Facchini, Livia Visai. 2010. In Vitro Enhancement of SAOS-2 Cell Calcified Matrix Deposition onto Radio Frequency Magnetron Sputtered Bioglass-Coated Titanium Scaffolds. *Tissue Engineering Part A* **16**:3, 995-1008. [Abstract] [Full Text HTML] [Full Text PDF] [Full Text PDF with Links]
29. S. Bertoldi, S. Farè, M. Denegri, D. Rossi, H. J. Haugen, O. Parolini, M. C. Tanzi. 2010. Ability of polyurethane foams to support placenta-derived cell adhesion and osteogenic differentiation: preliminary results. *Journal of Materials Science: Materials in Medicine* **21**, 1005-1011. [CrossRef]
30. Qiming Pang, Jean W. Zu, Geoffrey M. Siu, Ren-Ke Li. 2010. Design and Development of a Novel Biostretch Apparatus for Tissue Engineering. *Journal of Biomechanical Engineering* **132**, 014503. [CrossRef]
31. Giulia Gastaldi, Annalia Asti, Manuela Federica Scaffino, Livia Visai, Enrica Saino, Angela Maria Cometa, Francesco Benazzo. 2010. Human adipose-derived stem cells (hASCs) proliferate and differentiate in osteoblast-like cells on trabecular titanium scaffolds. *Journal of Biomedical Materials Research Part A* **9999A**, NA-NA. [CrossRef]
32. Lorenzo Fassina, Enrica Saino, Maria Gabriella Cusella De Angelis, Giovanni Magenes, Francesco Benazzo, Livia Visai. 2010. Low-Power Ultrasounds as a Tool to Culture Human Osteoblasts inside Cancellous Hydroxyapatite. *Bioinorganic Chemistry and Applications* **2010**, 1-8. [CrossRef]
33. F. Benazzo, G. Zanon. 2009. Stimolazione biofisica. *Archivio di Ortopedia e Reumatologia* **120**, 44-46. [CrossRef]
34. Ming-Tzu Tsai, Wan-Ju Li, Rocky S. Tuan, Walter H. Chang. 2009. Modulation of osteogenesis in human mesenchymal stem cells by specific pulsed electromagnetic field stimulation. *Journal of Orthopaedic Research* **27**:10.1002/jor.v27:9, 1169-1174. [CrossRef]
35. Lorenzo Fassina, Enrica Saino, Maria Sonia Sbarra, Livia Visai, Maria Gabriella Cusella De Angelis, Giuliano Mazzini, Francesco Benazzo, Giovanni Magenes. 2009. Ultrasonic and Electromagnetic Enhancement of a Culture of Human SAOS-2 Osteoblasts Seeded onto a Titanium Plasma-Spray Surface. *Tissue Engineering Part C: Methods* **15**:2, 233-242. [Abstract] [Full Text HTML] [Full Text PDF] [Full Text PDF with Links]
36. M. Zanetta, N. Quirici, F. Demarosi, M.C. Tanzi, L. Rimondini, S. Farè. 2009. Ability of polyurethane foams to support cell proliferation and the differentiation of MSCs into osteoblasts. *Acta Biomaterialia* **5**, 1126-1136. [CrossRef]
37. Jen-Chang Yang, Sheng-Yang Lee, Chi-An Chen, Che-Tong Lin, Chang-Chih Chen, Haw-Ming Huang. 2009. The role of the calmodulin-dependent pathway in static magnetic field-induced mechanotransduction. *Bioelectromagnetics* n/a-n/a. [CrossRef]
38. Hsin-Yi Lin, Ko-Hsien Lu. 2009. Repairing large bone fractures with low frequency electromagnetic fields. *Journal of Orthopaedic Research* n/a-n/a. [CrossRef]

39. Lorenzo Fassina, Enrica Saino, Maria Sonia Sbarra, Livia Visai, Maria Gabriella Cusella De Angelis, Giovanni Magenes, Francesco Benazzo. 2009. In vitro electromagnetically stimulated SAOS-2 osteoblasts inside porous hydroxyapatite. *Journal of Biomedical Materials Research Part A* **9999A**, NA-NA. [CrossRef]
40. Lorenzo Fassina, Enrica Saino, Livia Visai, Giulia Silvani, Maria Gabriella Cusella De Angelis, Giuliano Mazzini, Francesco Benazzo, Giovanni Magenes. 2008. Electromagnetic enhancement of a culture of human SAOS-2 osteoblasts seeded onto titanium fiber-mesh scaffolds. *Journal of Biomedical Materials Research Part A* **87A**:10.1002/jbm.a.v87a:3, 750-759. [CrossRef]
41. Guixin Shi, Ze Zhang, Mahmoud Rouabhia. 2008. The regulation of cell functions electrically using biodegradable polypyrrole–polylactide conductors. *Biomaterials* **29**, 3792-3798. [CrossRef]
42. Franco Benazzo, Matteo Cadossi, Francesco Cavani, Milena Fini, Gianluca Giavaresi, Stefania Setti, Ruggero Cadossi, Roberto Giardino. 2008. Cartilage repair with osteochondral autografts in sheep: Effect of biophysical stimulation with pulsed electromagnetic fields. *Journal of Orthopaedic Research* **26**:10.1002/jor.v26:5, 631-642. [CrossRef]
43. V. Grote, H. Lackner, C. Kelz, M. Trapp, F. Aichinger, H. Puff, M. Moser. 2007. Short-term effects of pulsed electromagnetic fields after physical exercise are dependent on autonomic tone before exposure. *European Journal of Applied Physiology* **101**, 495-502. [CrossRef]